Plant Biotechnology Journal
Open Access

Plant Biotechnology Journal (2024), pp. 1–14 doi: 10.1111/pbi.14544

Engineering a robust Cas12i3 variant-mediated wheat genome editing system

Wenxue Wang[1,2,†], Lei Yan[1,†], Jingying Li[1,2], Chen Zhang[1], Yubing He[1,2], Shaoya Li[1,2,*] and Lanqin Xia[1,2,*]

[1]*State Key Laboratory of Crop Gene Resources and Breeding, Institute of Crop Sciences (ICS), Chinese Academy of Agricultural Sciences (CAAS), Beijing, China*
[2]*National Nanfan Research Institute (Sanya), CAAS/Hainan Seed Industry Laboratory, Sanya, Hainan Province, China*

Received 9 September 2024;
revised 5 November 2024;
accepted 23 November 2024.
**Correspondence* (Tel 010-82105804; fax 010-82105804; email xialanqin@caas.cn (L.X.); Tel 010-82105921; fax 010-82105921; email lishaoya@caas.cn (S.L.))
†These authors contribute equally to this work.

Keywords: wheat (*Triticum aestivum* L.), CRISPR/Cas12i3, genome editing, T5 Exonuclease (T5E).

Summary

Wheat (*Triticum aestivum* L., 2*n* = 6*x* = 42, AABBDD) is one of the most important food crops in the world. CRISPR/Cas12i3, which belongs to the type V-I Cas system, has attracted extensive attention recently due to its smaller protein size and its less-restricted canonical 'TTN' protospacer adjacent motif (PAM). However, due to its relatively lower editing efficacy in plants and the hexaploidy complex nature of wheat, Cas12i3/Cas12i3-5M-mediated genome editing in wheat has not been documented yet. Here, we report the engineering of a robust Cas12i3-5M-mediated genome editing system in wheat through the fusion of T5 exonuclease (T5E) in combination with an optimised crRNA expression strategy (Opt). We first showed that fusion of T5E, rather than ExoI, to Cas12i3-5M increased the gene editing efficiencies by up to 1.34-fold and 3.87-fold, compared to Cas12i3-5M and Cas12i3 in HEK293T cells, respectively. However, its editing efficiency remains low in wheat. We then optimised the crRNA expression strategy and demonstrated that Opt-T5E-Cas12i3-5M could enhance the editing efficiency by 1.20- to 1.33-fold and 4.05- to 7.95-fold in wheat stable lines compared to Opt-Cas12i3-5M and Opt-Cas12i3, respectively, due to progressive 5′-end resection of the DNA strand at the cleavage site with increased deletion size. The Opt-T5E-Cas12i3-5M enabled an editing efficiency ranging from 60.71% to 90.00% across four endogenous target genes in stable lines of three elite Chinese wheat varieties. Together, the developed robust Opt-T5E-Cas12i3-5M system enriches wheat genome editing toolkits for either biological research or genetic improvement and may be extended to other important polyploidy crop species.

Introduction

Common wheat (*Triticum aestivum*, 2*n* = 6*x* = 42, AABBDD) is one of the most important staple food crops in the world. Despite that wheat production has significantly increased over the past decades, wheat production will face unprecedented challenges following global climate warming, frequent occurrences of extreme weather, increasing world population, and water shortages in arid and semi-arid lands. Furthermore, undue applications of diverse fertilisers and pesticides are exacerbating environmental pollution and ecological deterioration. To ensure global food and ecosystem security, it is essential to enhance the resilience of wheat production while minimising environmental pollution by using cutting-edge technologies such as genome editing. However, the relatively lower transformation efficiency, the hexaploidy genome, and the gene redundancy nature of wheat complicate its genome editing for either biological research or genetic improvement.

CRISPR/Cas12i3, which belongs to the type V-I Cas system, has attracted extensive attentions recently due to its smaller protein size and its less restricted canonical 'TTN' protospacer adjacent motifs (PAM) and expands the genome editing scope, compared to the widely used LbCas12a/AsCas12a and their orthologs with the canonical PAM of 'TTTV', and the widely used SpCas9 with the canonical PAM of 'NGG', and Cas12a's ancestors IsDra2 and IsDge10 with the TAM of 'TTGAT' and 'TTAT', respectively (Hui *et al.*, 2024; Karmakar *et al.*, 2024; Li *et al.*, 2018, 2019, 2021a; Ma *et al.*, 2024; Schindele and Puchta, 2020; Tang *et al.*, 2017; Wang *et al.*, 2021; Wolter and Puchta, 2019; Xin *et al.*, 2024; Zhang *et al.*, 2023b, 2024; Zhong *et al.*, 2018; Zhou *et al.*, 2023). Besides, in comparison with other smaller Cas12 proteins, such as Cas12f and Cas12j2, Cas12i3 exhibits relatively higher editing efficiency and is compatible with a shorter crRNA (Bigelyte *et al.*, 2021; Liu *et al.*, 2022; Lv *et al.*, 2024). Like LbCas12a/AsCas12a, Cas12i3 produces double-strand breaks (DSBs) with 5′-staggered ends (Duan *et al.*, 2024; Lv *et al.*, 2024). Although SpCas9 and LbCas12a/AsCas12a have dominated the genome editing field over the past 10 years (Li *et al.*, 2018, 2019, 2020, 2021b,2021c, 2023, 2024; Luo *et al.*, 2021; Ma *et al.*, 2024; Sun *et al.*, 2017; Tang *et al.*, 2017; Wang *et al.*, 2021; Zhang *et al.*, 2021; Zhong *et al.*, 2018), the application of Cas12i3 in plant genome editing has rarely been reported. The editing activity of Cas12i3 is relatively lower in both mammalian cells and plants (Huang *et al.*, 2020; Zhang *et al.*, 2020a, 2023a). To improve the editing efficiency of CRISPR/Cas12i3, Duan et al. rationally designed the key residues in Cas12i3 that were potentially involved in the interaction between Cas12i3, crRNA, and its substrate DNA, and achieved a highly efficient Cas12i3-5M (S7R/D233R/D267R/N369R/S433R) variant. In rice, Cas12i3-5M exhibited an increased

Please cite this article as: Wang, W., Yan, L., Li, J., Zhang, C., He, Y., Li, S. and Xia, L. (2024) Engineering a robust Cas12i3 variant-mediated wheat genome editing system. *Plant Biotechnol. J.*, https://doi.org/10.1111/pbi.14544.

editing efficiency of up to 5-fold compared with wild-type Cas12i3, with averaged editing efficiency reaching up to 75% (Duan *et al*., 2024), opening a roadmap for the potential application of Cas12i3-5M in crop genome editing. However, wheat is a hexaploid species possessing three homoeologous genomes (2*n* = 6*x* = 42, AABBDD). Given the fact that Cas12i3 or Cas12i3-5M generally induces the 5′-overhangs at the PAM-distal position (Duan *et al*., 2024), and the compatible single-strand overhangs may result in re-ligation of nicks in both DNA strands without indels (insertion and deletion) through the error-free non-homologous end joining (eNHEJ) repair pathway, which potentially compromises the editing performance of Cas12i3/Cas12i3-5M in wheat. Indeed, this phenomenon had been observed in wheat genome editing upon using the LbCas12a, which also cuts at the PAM-distal position and usually induces similar 5′ staggered overhangs, displayed a relatively lower editing efficiency in comparison to SpCas9 (Wang *et al*., 2021). To date, the Cas12i3/Cas12i3-5M-mediated wheat genome editing system has not been documented yet.

Exonucleases have been applied in combination with the CRISPR/Cas9 reagent to enhance its editing efficacy (Clements *et al*., 2017; Zhang *et al*., 2020b). Exonucleases (Exo) catalyse the excision of nucleoside monophosphates from the 3′ or 5′ DNA termini (Clements *et al*., 2017; Garforth and Sayers, 1997; Shevelev *et al*., 2002; Tran *et al*., 2004). Co-expression of the CRISPR/Cas9 reagent with 3′−5′ exonuclease ExoI (Clements *et al*., 2017) or fusion with a 5′−3′ exonuclease T5E (Wu *et al*., 2020; Zhang *et al*., 2020b), resulted in increased insertion and deletion (indel) frequencies. We reasoned that fusion of DNA end-processing enzymes, such as ExoI and T5E, may generate DNA recessions that prevent the re-ligation/repair of target DNA at the cleavage sites through the cellular error-free NHEJ repair pathway and thereby direct the DNA repair into the error-prone NHEJ pathway (Budman *et al*., 2007; Gu *et al*., 2007; Moore and Haber, 1996), offering an alternative to improve the editing performance of the members of the Cas12 family, including Cas12i3/Cas12i3-5M, which usually produce 5′-overhangs. However, whether ExoI and T5E could be used to improve the editing efficiency of Cas12i3/Cas12i3-5M remains to be investigated.

Here, we report the engineering of a robust Cas12i3-5M-mediated genome editing system in wheat through fusion of T5E and combined with an optimised crRNA expression strategy, which is referred to as Opt-T5E-Cas12i3-5M. We first demonstrated that fusion of T5E, rather than ExoI, to the N-termini of the Cas12i3-5M could significantly improve the editing efficacy in HEK293 cells. Furthermore, T5E-Cas12i3-5M showed even superior editing performance compared to LbCas12a. We then performed wheat genome editing by using two different crRNA expression strategies. Our results indicated that when using an optimised crRNA expression strategy (Opt) and choosing *bar* as a selection marker gene, the fusion of T5E to Cas12i3-5M (Opt-T5E-Cas12i3-5M) could significantly increase the editing efficiencies by up to 7.95-fold and 1.33-fold in comparison to Opt-Cas12i3 and Opt-Cas12i3-5M, respectively, due to progressive 5′-end resection of the DNA strand at the cleavage site with increased deletion size. The Opt-T5E-Cas12i3-5M could enable an average editing efficiency of up to 88.99% at the tested four endogenous loci in stable lines of three elite Chinese wheat varieties. The developed robust Opt-T5E-Cas12i3-5M system not only expands the editing scope and enriches the wheat genome editing toolkits but also will facilitate its application in genome editing of wheat as well as other agriculturally important polyploidy crop plants, either for biological research or genetic improvement.

Results

T5E-Cas12i3-5M significantly increased editing efficiency in HEK293T cells

Like LbCas12a (Zetsche *et al*., 2015), Cas12i3 or Cas12i3-5M usually generates similar 5′-staggered ends at the double DNA break (DSB), which can potentially be repaired by the error-free NHEJ pathway by Watson-Crick base pairing and thus will lead to decreased genome editing efficiency (Figure 1a). Fusion of an exonuclease I (ExoI) to SpCas9 resulted in increased mutation efficiency in zebrafish embryos (Clements *et al*., 2017). Furthermore, fusion of T5E, a 5′ → 3′ exonuclease, to either Cas12a or Cas9 could direct the cellular DNA repair pathway into the error-prone NHEJ pathway, enabling higher indel efficiency in human cells and rice plants (Clements *et al*., 2017; Wu *et al*., 2020; Zhang *et al*., 2020b). Wheat is a hexaploid crop species with a complex AABBDD genomic background. To enable Cas12i3-5M-mediated genome editing in wheat and further improve its editing efficacy, we assumed that fusing an exonuclease, either ExoI or T5E, to Cas12i3-5M at its N-termini could lead to the progressive 3′- or 5′-end resection of DNA strands at the cleavage site, increase the occurrence of the error-prone NHEJ DNA repair pathway, and thus enhance its indel frequency. Given that the transient wheat protoplast transformation is usually not repeatable and somehow not reliable, to test this hypothesis, we first evaluated the activities of these Cas12i3 variants in mammalian HEK293T cells. We fused either ExoI or T5E to the N-terminus of Cas12i3-5M with a 32-amino acid linker to generate ExoI-Cas12i3-5M, and T5E-Cas12i3-5M constructs (Figure 1b). We tested and compared the editing performances of Cas12i3, Cas12i3-5M, ExoI-Cas12i3-5M, T5E-Cas12i3-5M and the widely used LbCas12a nuclease at three wheat targets in HEK293T cells, respectively. As shown in Figure 1c, these three wheat targets include one target from *TaARE1*-D; knock-out of *TaARE1*-D results in wheat with increased nitrogen use efficacy and improved yield under nitrogen-limiting conditions (Zhang *et al*., 2021), one target from *TaHRC-D*, whose knock-out leads to improved wheat head scab resistance (Su *et al*., 2019), and the other one from *TaSBEIIa*, which plays an important role in determining starch composition, structure, and properties in wheat; knock-out of this gene results in high-amylose wheat (Li *et al*., 2021b). We also designed a fluorescent reporter system that detected the green fluorescent protein (EGFP) signal intensity activated by Cas-mediated dsDNA cleavage or DSB (Figure 1d). This system relied on the co-transfection of one plasmid harbouring a nuclear localisation signal (NLS)-tagged Cas protein, its crRNA, and a gene encoding BFP (Tong *et al*., 2023), fused to Cas protein (Figure 1b), and another target plasmid expressing mCherry (Tong *et al*., 2023) and the activatable EGFxxFP cassette (Figure 1b) (Yang et al., 2016), in which the three wheat targets (Figure 1c) were inserted with their corresponding PAMs in a tandem array (target plasmid in Figure 1b) in an architecture of EGxx-target sites-xxFP. In theory, EGFP was activated by Cas-mediated DSB and single-strand annealing (SSA)-mediated repair (Figure 1d).

As determined by fluorescence-activated cell sorting (FACS) analyses, Cas12i3 exhibits a relatively low average editing efficiency of 21.01 ± 1.83%, 21.38 ± 2.34%, 20.69 ± 1.76% at *TaARE-D*, *TaHRC-D* and *TaSBEIIa* targets, respectively, whereas

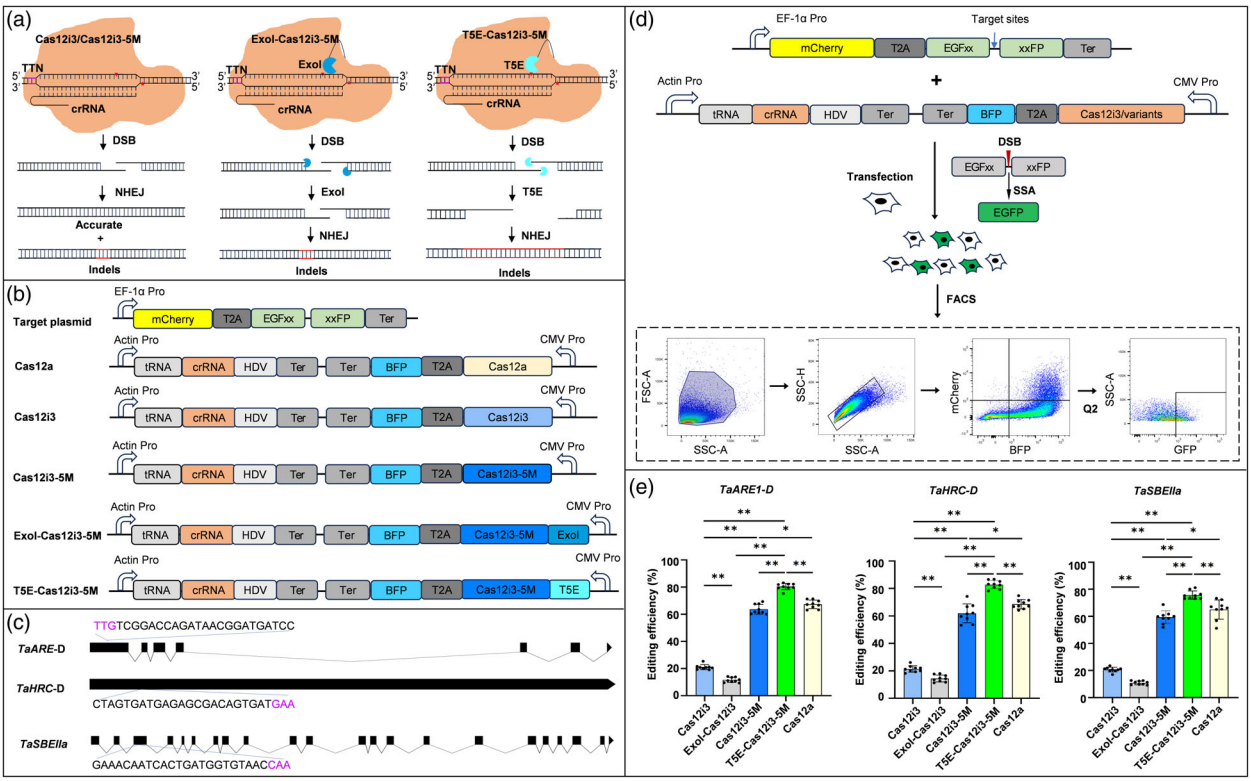

Figure 1 Schematic diagrams of Cas12a (LbCas12a)/Cas12i3/Cas12i3-5M/ExoI-Cas12i3-5M/T5E-Cas12i3-5M and their performances in HEK293T cells. (a) Illustration of the Cas12a/Cas12i3/Cas12i3-5M, ExoI-Cas12i3/Cas12i3-5M and T5E-Cas12i3/Cas12i3-5M systems and corresponding DNA repair pathways. Cas12i3 generates fully compatible sticky ends, which are mainly repaired by the precise non-homologous end joining (NHEJ) pathway and thus will not contribute to insertion and deletion (indel) efficiency. ExoI is a 3′ → 5′ ssDNA exonuclease. T5 Exonuclease-fused Cas12i3 can degrade the single-strand DNA overhang after cleavage and could bias the cellular repair pathway mainly into imprecise NHEJ, which will result in the enhancement of indel efficiency. (b) Schematic diagrams of Cas12a, Cas12i3, Cas12i3-5M, ExoI-Cas12i3-5M and T5E-Cas12i3-5M. Cas12i3, Cas12i3-5M, ExoI-Cas12i3-5M and T5E-Cas12i3-5M are fused with BPF driven by the CMV promotor, whereas the tRNA-crRNA-HDV is expressed under the control of the chicken actin promoter. ExoI, Exonuclease I; T5E, T5 Exonuclease; Ter, Terminator. (c) The structures of *TaARE1-D*, *TaHRC-D* and *TaSBEIIa*. Exon regions are shown as blank boxes, and the PAM sites (5′-TTN-3′) are highlighted in pink. (d) Schematics of the EGFxxFP reporter system for detecting the editing efficiency of Cas12a/Cas12i3/Cas12i3-5M/ExoI-Cas12i3-5M/T5E-Cas12i3-5M in HEK293T cells. PAM-Target sequences are inserted inside the eGFP to disrupt its fluorescence. Targeted cleavage in the inserted sequence can restore EGFP fluorescence through single-strand annealing (SSA)-mediated DNA repair between the repeats of EGFxxFP. P4190 and S4254 in this system can constitutively express mCherry and BFP fluorescence, respectively. Editing efficiency is assessed by determining the ratio of EGFP+ cells over mCherry+ and BFP+ cells. FACS, Fluorescence Activated Cell Sorter. (e) The performances of Cas12a, Cas12i3, Cas12i3-5M, ExoI-Cas12i3-5M and T5E-Cas12i3-5M in HEK293T cells. Bar plots showing the on-target DNA base editing frequencies of Cas12a, Cas12i3, Cas12i3-5M, ExoI-Cas12i3-5M and T5E-Cas12i3-5M in HEK293T cells, respectively. The editing outcomes are calculated based on three independent biological replicates (each replicate was performed with 3 repeats). **, $P < 0.01$; *, $0.01 < P < 0.05$.

Cas12i3-5M induced an improved average editing efficiency of 63.70 ± 3.59%, 61.92 ± 6.76%, 59.37 ± 4.72% at the *TaARE-D*, *TaHRC-D* and *TaSBEIIa* targets, respectively (Figure 1e, Table S2). In comparison with Cas12i3, Cas12i3-5M improved the editing efficiency by 3.03-fold at *TaARE1-D* (63.70%/21.01%), 2.90-fold at *TaHRC-D* (61.92%/21.38%) and 2.87-fold at *TaSBEIIa* (59.37%/20.69%) (Figure 1e, Table S2), respectively, which was in consistence with a previous report (Duan *et al.*, 2024). However, ExoI-Cas12i3-5M showed decreased editing efficiencies of 11.66 ± 1.83%, 14.47 ± 2.49% and 10.86 ± 1.38% at the *TaARE-D*, *TaHRC-D* and *TaSBEIIa* targets, respectively, which were even lower than the wild type Cas12i3 (Figure 1e). Notably, T5E-Cas12i3-5M exhibited a significantly higher editing efficiency than Cas12i3 and Cas12i3-5M, with the average editing efficiency of 80.44 ± 2.34%, 82.80 ± 3.01% and 75.72 ± 3.03% at the *TaARE-D*, *TaHRC-D* and *TaSBEIIa* targets (Figure 1e, Table S2), respectively. In comparison with Cas12i3 and Cas12i3-5M, T5E-Cas12i3-5M significantly increased gene editing efficiencies by 3.82-fold (80.44%/21.01%), 3.87-fold (82.80%/21.38%), 3.66-fold (75.72%/20.69%), and 1.26-fold (80.44%/63.70%), 1.34-fold (82.80%/61.92%), 1.28-fold (75.72%%/59.37%) at *TaARE-D*, *TaHRC-D* and *TaSBEIIa* targets, respectively (Table S2). In addition, our results also demonstrated that LbCas12a exhibited an average editing efficiency of 67.33 ± 3.10%, 68.56 ± 3.31% and 65.04 ± 7.05% at the *TaARE-D*, *TaHRC-D* and *TaSBEIIa* targets, respectively (Figure 1e, Table S2), higher than Cas12i3-5M but significantly lower than T5E-Cas12i3-5M (Figure 1e, Table S2). These results demonstrated that T5E-Cas12i3-5M enables robust genome editing in mammalian cells. Given that Cas12i3, Cas12i3-5M and T5E-Cas12i3-5M exhibited a considerable editing efficiency, we next chose them for subsequent wheat genome editing to further evaluate their performances in wheat stable lines, respectively.

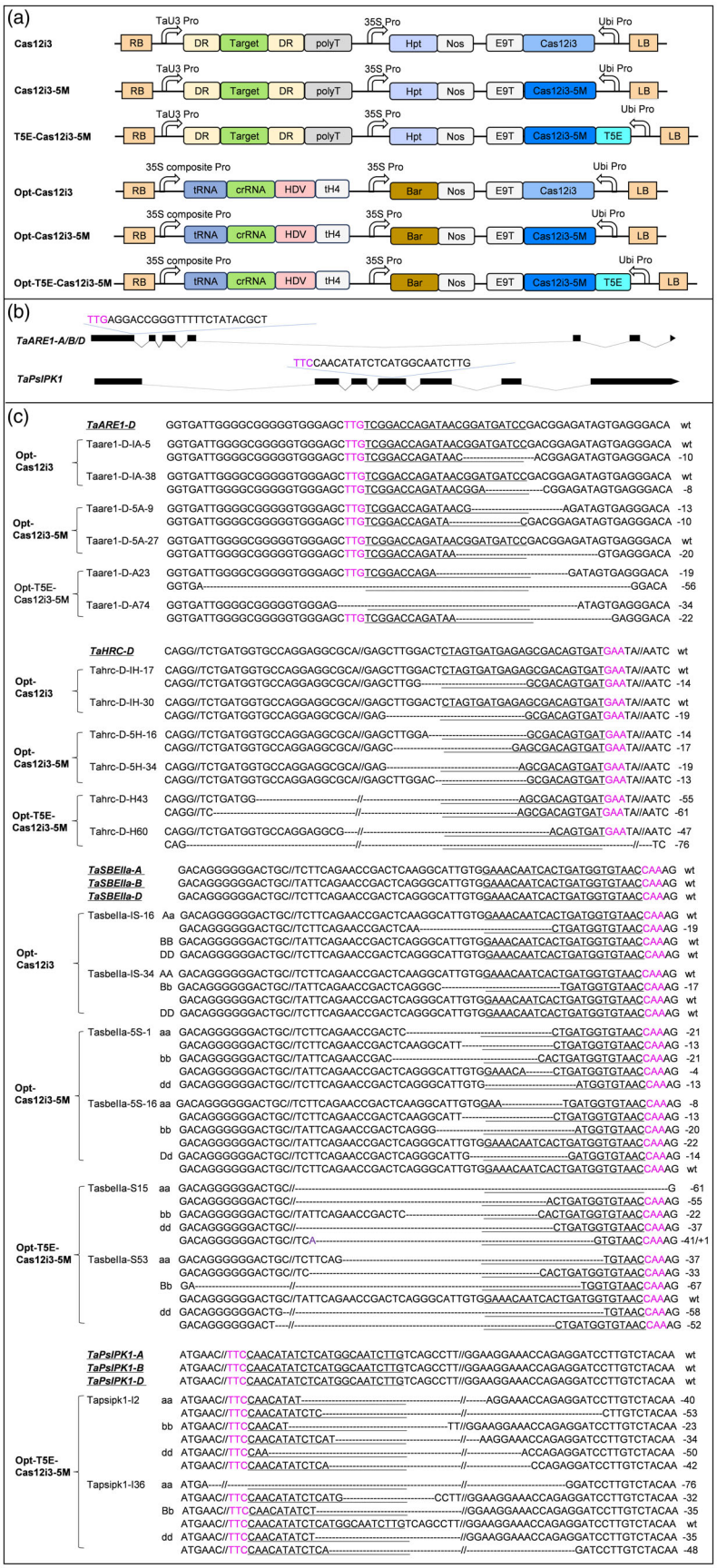

Figure 2 Schematic presentations of the T-DNA structures of Cas12i3, Cas12i3-5M, T5E-Cas12i3-5M, and their optimised versions, respectively, and sequencing results of two representative mutant lines derived from each corresponding optimised version in the T_0 generation. (a) Schematic diagrams of Cas12i3, Cas12i3-5M, T5E-Cas12i3-5M, Opt-Cas12i3, Opt-Cas12i3-5M and Opt-T5E-Cas12i3-5M. In Cas12i3, Cas12i3-5M and T5E-Cas12i3-5M, the Cas12i3, Cas12i3-5M and T5E-Cas12i3-5M are driven by a maize *Ubiquitin* promotor (*Ubi*), and the DR-crRNA is expressed under the control of the *OsU3* promoter and terminated with 'TTTTTTT', and the *hptII* is used as a selection marker gene. In Opt-Cas12i3, Opt-Cas12i3-5M and Opt-T5E-Cas12i3-5M, the 35S composite promoter (35S-CmYLCV-U6) is used to drive the expression of a tRNA-crRNA-HDV array and *bar* gene as a selection marker. T5E, T5 Exonuclease. (b) The gene structures of *TaARE1* and *TaPslPK1*. Exon regions are shown as blank boxes, and the PAM sites (5′-TTN-3′) are highlighted in pink. (c) Sequencing results of the two representative mutant lines of TaARE1-D-crRNA, TaHRC-D-crRNA, TaSBEIIa-crRNA and TaPslPK1-crRNA were derived from each corresponding optimised version in the T_0 generation, respectively. The PAM motifs are highlighted in pink, target sequences are underlined, and the dashes indicate deletions.

T5E-Cas12i3-5M induced targeted mutagenesis in wheat stable lines, but its efficacy remains very lower

To further evaluate the editing performances of Cas12i3, Cas12i3-5M and T5E-Cas12i3-5M in wheat stable lines and test whether they could induce efficient targeted mutagenesis, we cloned Cas12i3, Cas12i3-5M and T5E-Cas12i3-5M into an all-in-one vector, pHUE411, in which a conventional *Pol* III promoter, *TaU3*, was used to drive the DR-target-DR array (DR, directed repeat), and the selection marker gene *hpt* was driven by the *35S* promoter, respectively (Figure 2a). We chose the endogenous *TaARE1* as the target gene (Figure 2b, Table S3). We then transformed the Cas12i3, Cas12i3-5M and T5E-Cas12i3-5M constructs targeting *TaARE1* (Figure 2a) into an elite Chinese wheat variety, *cv* Zhengmai 7698 (ZM7698), which is widely planted in the central Huanghuai region in China, through *Agrobacterium*-mediated transformation to generate stable lines. Unexpectedly, all three of these constructs exhibited a much lower editing efficiency with no edited lines generated by Cas12i3 and Cas12i3-5M at all (Table 1). T5E-Cas12i3-5M enabled the editing at *TaARE1* loci at the efficiencies of 10.00% (1/10), 20.00% (1/5) and 33.33% (2/6), respectively, with an average editing efficiency of 21.11 ± 11.70% (Table 1). In the four edited wheat lines, line *Taare1-92* contained the heterozygous mutations in A and D subgenomes, respectively, and line *Taare1-443* only contained a heterozygous mutation in A subgenome, and line *Taare1-323* and *TaARE1-409* only contained the heterozygous mutations in B genome (Table S4). Together, although T5E-Cas12i3-5M enables detectable genome editing in wheat stable lines, the editing efficiency is relatively lower and needs to be further optimised.

Opt-T5E-Cas12i3-5M enables robust genome editing in wheat stable lines

It was reported that the 35S-CmYLCV-U6 composite promoter is more efficient than the *Pol* III promoter (*U3* or *U6*) in CRISPR/Cas-mediated prime editing in rice (Jiang *et al*., 2020, 2022). In addition, tRNA and HDV ribozymes flanking the entire crRNA array were more efficient than the DR strategy (Jiang *et al*., 2020). To further improve the editing efficiency of Cas12i3 and its variants in wheat, we optimised the constructs as follows: (1) Replacing the promoter *TaU3* with a composite promoter (35S-CmYLCV-U6) to drive the expression of a tRNA-crRNA-HDV array; (2) using *bar* as a selection gene in wheat tissue culture. We finally generated the Opt-Cas12i3, Opt-Cas12i3-5M and Opt-T5E-Cas12i3-5M constructs, respectively (Figure 2a).

We then evaluated the editing performances of Opt-Cas12i3, Opt-Cas12i3-5M and Opt-T5E-Cas12i3-5M at three endogenous target genes, *TaARE-D*, *TaHRC-D* and *TaSBEIIa* targets in wheat stable lines, respectively (Figures 1c, 2a, Table 1). For Opt-Cas12i3, at the *TaARE-D* locus, the editing efficiencies were 11.76% (2/17), 9.10% (1/11) and 16.67% (3/18) in three biological repeats, respectively, with an average editing efficiency of 12.51 ± 3.84% (Table 1). All six T_0 mutant lines had heterozygous mutations in the D subgenome of the *TaARE1* gene (Figure 2c, Table S5). At the *TaHRC-D* locus, the editing efficiencies were 10.00% (1/10), 11.11% (1/9) and 12.50% (1/8) in three biological repeats, respectively, with an average editing efficiency of 11.20 ± 1.25% (Table 1). All these obtained three T_0 mutant lines carried heterozygous mutations in the D subgenome (Figure 2c, Table S6). At *TaSBEIIa*, the editing efficiencies were 16.67% (2/12), 20.00% (3/15) and 18.18% (2/11) in three biological repeats, respectively, with an average editing efficiency of 18.28 ± 1.67% (Table 1). In these 7 T_0 mutant lines, one line carried a heterozygous mutation only in the A subgenome, and 4 lines carried heterozygous mutations in B subgenome, and one line had a heterozygous mutation in the D subgenome, and one line had mutations both in the A and D subgenomes (Figure 2c, Table S7).

Opt-Cas12i3-5M enabled more efficient gene editing efficiency at all three targets in comparison with Cas12i3 (Table 1). For the *TaARE-D* target, the editing efficiencies were 58.33% (7/12), 57.14% (4/7) and 57.14% (8/14) in three transformation repeats, respectively, with the average editing efficiency of 57.54 ± 0.69% (Table 1). Among these edited lines, 12 out of 19 (63.19%) mutants had biallelic or homozygous mutations, and the remaining seven were heterozygous or chimeric (Figure 2c, Table S5). For the *TaHRC-D* target, the editing efficiencies were 66.67% (8/12), 62.50% (5/8) and 71.43% (15/21) in three transformation repeats, respectively, with an average editing efficiency of 66.87 ± 4.47% (Table 1). Among the 28 T_0 mutant lines, 53.57% (15/28) lines had either homozygous or biallelic mutations in the D subgenome and the remaining 13 were heterozygous or chimeric lines (Figure 2c, Table S6). For the *TaSBEIIa* target, the editing efficiencies were 58.33% (7/12), 64.71% (11/17) and 46.67% (7/15) in three transformation repeats, respectively, with an average editing efficiency of 56.57 ± 9.15% (Table 1). Among the obtained 25 independent mutant lines, eight lines had mutations in only one subgenome, among which one line had a chimeric mutation in *TaSBEIIa-A*, and 3 lines had biallelic or heterozygous mutations in *TaSBEIIa-B*, and four lines had biallelic, heterozygous, or chimeric mutations in *TaSBEIIa-D* (Table S7). Four out of 25 lines had mutations in both two of the three sub-genomes. Among these four lines, one line had mutations both in *the TaSBEIIa-A* and *TaSBEIIa-B* genomes, and one line carried mutations in both in *TaSBEIIa-B* and *TaSBEIIa-D*, and two lines had mutations in both in the *TaSBEIIa-A* and *TaSBEIIa-D* genomes (Figure 2c, Table S7). All the remaining 13

Table 1 The editing performances of Cas12i3, Cas12i3-5M, T5E-Cas12i3-5M and their optimized versions in wheat stable lines

Targets	Vectors	Donor Variety	No. of embryos	Recovered lines	No. of independent transgenic lines	No. of Independent mutant lines	Editing efficiency (%)	Average editing efficiency (%)
TaARE1-A/B/D	Cas12i3	ZM7698	714	59	11	0	0.00	0.00
			572	41	10	0	0.00	
	Cas12i3-5M	ZM7698	158	55	5	0	0.00	0.00
			243	87	7	0	0.00	
	T5E-Cas12i3-5M	ZM7698	387	146	10	1	10.00	21.11 ± 11.70
			476	254	5	1	20.00	
			513	225	6	2	33.33	
TaARE1-D	Opt-Cas12i3	ZM7698	181	21	17	2	11.76	12.51 ± 3.84[c]
			107	14	11	1	9.10	
			171	18	18	3	16.67	
	Opt-Cas12i3-5M	ZM7698	156	12	12	7	58.33	57.54 ± 0.69[b]
			160	7	7	4	57.14	
			181	15	14	8	57.14	
	Opt-T5E-Cas12i3-5M	ZM7698	269	48	46	30	65.22	63.25 ± 2.31[a]
			277	48	47	30	63.83	
			192	28	28	17	60.71	
TaHRC-D	Opt-Cas12i3	ZM7698	70	11	10	1	10.00	11.20 ± 1.25[c]
			81	11	9	1	11.11	
			73	8	8	1	12.50	
	Opt-Cas12i3-5M	ZM7698	98	12	12	8	66.67	66.87 ± 4.47[b]
			95	9	8	5	62.50	
			105	21	21	15	71.43	
	Opt-T5E-Cas12i3-5M	ZM7698	187	24	19	17	89.47	88.99 ± 1.32[a]
			202	23	20	18	90.00	
			124	17	16	14	87.50	
TaSBEIIa	Opt-Cas12i3	ZM7698	70	12	12	2	16.67	18.28 ± 1.67[c]
			113	17	15	3	20.00	
			91	11	11	2	18.18	
	Opt-Cas12i3-5M	ZM7698	181	12	12	7	58.33	56.57 ± 9.15[b]
			174	17	17	11	64.71	
			185	17	15	7	46.67	
	Opt-T5E-Cas12i3-5M	ZM7698	222	11	11	8	72.73	73.98 ± 3.35[a]
			175	10	9	7	77.78	
			107	8	7	5	71.43	
TaPslPK1	Opt-T5E-Cas12i3-5M	ZM7698	156	14	13	8	61.54	60.95 ± 1.91
			241	19	17	10	58.82	
			187	16	16	10	62.50	
TaSBEIIa	Opt-T5E-Cas12i3-5M	ZM1860	73	11	10	7	70.00	75.00 ± 7.07
			78	5	5	4	80.00	
TaSBEIIa	Opt-T5E-Cas12i3-5M	ZS9170	78	10	9	7	77.78	76.39 ± 1.97
			70	5	4	3	75.00	

The values of average editing efficiency are shown as mean ± SD. Different letters denote significant differences ($P < 0.05$) as determined by analysis of variance in each target gene.

mutant lines carried mutations in *TaSBEIIa-A*, *TaSBEIIa-B* and *TaSBEIIa-D* simultaneously (Figure 2c, Table S7). Compared with Opt-Cas12i3, Opt-Cas12i3-5M increased the gene editing efficiencies by 4.60-fold (57.54%/12.51%), 5.97-fold (66.87%/11.20%) and 3.09-fold (56.57%/18.28%) at the *TaARE-D*, *TaHRC-D* and *TaSBEIIa* targets, respectively (Table 1). These results indicated that Opt-Cas12i3-5M was more efficient in wheat genome editing compared with Opt-Cas12i3.

Consistent with the performance of T5E-Cas12i3-5M in HEK293T cells (Figure 1e), Opt-T5E-Cas12i3-5M outperformed Opt-Cas12i3-5M and enabled more robust genome editing with the average efficiencies ranging from 63.25% to 88.99% in wheat stable lines (Table 1). For the *TaARE-D* target, the editing efficiencies were 65.22% (30/46), 63.83% (30/47) and 60.71% (17/28) in three transformation repeats, respectively, with an average editing efficiency of 63.25 ± 2.31% (Table 1). Among these obtained 77 independent mutant lines, 32 out of 77 (41.56%) mutants had either biallelic or homozygous mutations, and the remaining 45 were heterozygous or chimeric (Figure 2c, Table S5). For the *TaHRC-D* target, the editing efficiencies were 89.47% (17/19), 90.00% (18/20) and 87.50% (14/16) in three transformation repeats, respectively, with an average editing

efficiency of 88.99 ± 1.08% (Table 1). Among the obtained 49 independent mutant lines, 67.35% (33/49) lines had homozygous or biallelic mutations in the D subgenome, and the remaining 16 were heterozygous or chimeric lines (Figure 2c, Table S6). For the *TaSBEIIa* target, the editing efficiencies were 72.73% (8/11), 77.78% (7/9) and 71.43% (5/7) in three transformation repeats, respectively, with an average editing efficiency of 73.98 ± 3.35% (Table 1). Among the obtained 20 independent mutant lines, nine lines had mutations in only one subgenome, among which five lines that had heterozygous or chimeric mutations in *TaSBEIIa-A*, and four lines that had either biallelic or heterozygous mutations in *TaSBEIIa-D* (Figure 2c, Table S7). Six out of 20 independent T_0 mutant lines had mutations in two of the three subgenomes, including five lines had mutations both in *TaSBEIIa-A* and *TaSBEIIa-B*, and one line had mutations both in *TaSBEIIa-A* and *TaSBEIIa-D* (Figure 2c, Table S7). All the remaining five independent mutant lines carried mutations in *TaSBEIIa-A*, *TaSBEIIa-B* and *TaSBEIIa-D* simultaneously (Figure 2c, Table S7). In comparison with Opt-Cas12i3-5M, Opt-T5E-Cas12i3-5M improved the genome editing efficiencies by 1.10-fold (63.25%/57.54% at *TaARE1-D*), 1.33-fold (88.99%/66.87% at *TaHRC-D*) and 1.31-fold (73.98%/56.57% at *TaSBEIIa*), respectively (Table 1).

To test the feasibility of Opt-T5E-Cas12i3-5M in editing other endogenous genes, we further edited *TaPsIPK1* in ZM7698 through *Agrobacterium*-mediated transformation (Figure 2a,b). *TaPsIPK1*, encoding a wheat receptor-like cytoplasmic kinase, is an effector of *Puccinia striiformis* f. sp. *tritici* (*Pst*), and inactivation of *TaPsIPK1* in wheat confers wheat plants broad-spectrum resistance against *Pst* (Wang *et al.*, 2022). We achieved a series of edited lines with the editing efficiencies of 61.54% (8/13), 58.82% (10/17) and 62.50% (10/16) in three transformation repeats, respectively. The average editing efficiency was 60.95 ± 1.91% (Table 1). Among the obtained 28 independent mutant lines, one line had a mutation in *TaPsIPK1-A*, and two lines had mutations in both *TaPsIPK1-A* and *TaPsIPK1-B*, and three lines had mutations both in *TaPsIPK1-A* and *TaPsIPK1-D* (Figure 2c, Table S8). All the remaining 22 lines (22/28, 78.57%) mutant lines carried simultaneous mutations in the *TaPsIPK1-A*, *TaPsIPK1-B* and *TaPsIPK1-D* subgenomes, respectively (Figure 2c, Table S8). This result further illustrates that Opt-T5E-Cas12i3-5M indeed enabled robust genome editing in hexaploidy wheat.

Opt-T5E-Cas12i3-5M induces a higher proportion of larger deletions in the edited wheat lines

Opt-T5E-Cas12i3-5M not only enhanced the significantly improved genome editing efficacy but also induced a higher proportion of larger deletions in the edited wheat stable lines. For example, at the *TaARE1*-D target, by Opt-Cas12i3, we obtained six independent edited lines in T_0 transformants, and all the indels were 11–20 bp deletions (Figure 3a, Table S9). By Opt-Cas12i3-5M, we obtained 19 independent edited lines in T_0 transformants and 100% indels were 1–30 bp deletions followed with 2 bp random insertion or base substitution in a few events (Figure 3a, Table S9). By Opt-T5E-Cas12i3-5M, we obtained 77 independent edited lines in T_0 transformants, among which 55.36% were 1–30 bp deletions followed by short random insertion, 39.55% were 31–100 bp deletions, and 5.09% were larger than 100 bp, with the largest deletion being 182 bp in length (Figure 3a, Table S9).

At *TaHRC-D* target, we obtained 3 independent edited lines in T_0 transformants by Opt-Cas12i3, and all the indels were 11–20 bp deletions (Figure 3b, Table S9). By Opt-Cas12i3-5M, we obtained 28 independent edited lines with all the indels being 1–50 bp deletions, among which 92.89% indels being 1–30 bp deletions, and 7.11% indels being 31–50 bp deletions (Figure 3b, Table S9). By Opt-T5E-Cas12i3-5M, we obtained 49 independent edited lines with 39.87% indels were 1–30 bp deletions followed with short random insertions, and 51.72% of the indels being 31–100 bp deletions, and 8.41% of the deletions being larger than 100 bp, with the largest deletion being 249 bp in length (Figure 3b, Table S9).

Common wheat is a hexaploid species. There are three homologues located in the A, B and D subgenomes, respectively. To accurately assess the deletion types of *TaSBEIIa*, we treated each homologue on one subgenome as a target locus, because the occurrence of deletions in one homologue on one subgenome didn't necessarily mean the same deletions happened on the other two subgenomes. For *TaSBEIIa-A*, all the indels induced by Opt-Cas12i3 were 11–20 bp deletions (Figure 3c), whereas all indels induced by Opt-Cas12i3-5M were 1–40 bp deletions following with 2 bp random insertions or base substitutions in a few events, among which 96.67% indels were 1–30 bp deletions, and 3.33% indels were 31–40 bp deletion (Figure 3c, Table S9). Opt-T5E-Cas12i3-5M induced a higher proportion of larger deletions. Among the obtained independent mutant lines by Opt-T5E-Cas12i3-5M, 32.59% were 1–30 bp deletions, 63.71% were 31–100 bp deletions, and 3.70% were larger than 100 bp, with the largest deletion being 209 bp in length (Figure 3c, Table S9). For *TaSBEIIa-B*, all indels generated by Opt-Cas12i3 were 1–40 bp deletions, among which 66.67% indels were 31–40 bp deletions, accounting for 33.33%, whereas the deletions of 1–30 bp, 31–40 bp and 51–60 bp generated by Opt-Cas12i3-5M accounted for 94.29%, 2.38% and 3.33%, respectively (Figure 3d, Table S9). In consistency with the above results at other target loci, among all the indels induced by Opt-T5E-Cas12i3-5M, 52.38% were 1–30 bp deletions, 36.51% were 31–100 bp deletions, and 11.11% were larger than 100 bp (Figure 3d, Table S9). For *TaSBEIIa-D*, all indels induced by Opt-Cas12i3 were 1–20 bp deletions, whereas the indels induced by Opt-Cas12i3-5M were 93.10% 1–30 bp deletions, 3.45% were 31–60 bp deletions, and 3.45% were larger than 100 bp (Figure 3e, Table S9). Furthermore, among all the indels induced by Opt-T5E-Cas12i3-5M, 33.33% were 1–30 bp deletions and 66.67% were 31–100 bp, in which 16.67% were 91–100 bp deletions (Figure 3e, Table S9).

Opt-T5E-Cas12i3-5M also introduced a higher proportion of larger deletions after editing of three homologues of *TaPsIPK1*. For example, at *TaPsIPK1-A*, 18.77% of the indels induced by Opt-T5E-Cas12i3-5M were 1–30 bp deletions, and 63.71% were 31–100 bp deletions, and 17.52% were larger than 100 bp (Figure 3f, Table S9). At *TaPsIPK1-B*, 36.06% of the indels induced by Opt-T5E-Cas12i3-5M were 1–30 bp deletions, 51.02% were 31–100 bp deletions, and 12.92% were larger than 100 bp in length (Figure 3g, Table S9). At *TaPsIPK1-D*, 26.47% of the indels induced by Opt-T5E-Cas12i3-5M were 1–30 bp deletions, 56.36% were 31–100 bp deletions, and 17.17% of deletions were larger than 100 bp in length (Figure 3h, Table S9).

Overall, compared with Opt-Cas12i3 and Opt-Cas12i3-5M, Opt-T5E-Cas12i3-5M not only enabled a significantly higher editing efficiency in wheat stable lines but also induced a higher proportion of larger deletions in wheat genome editing.

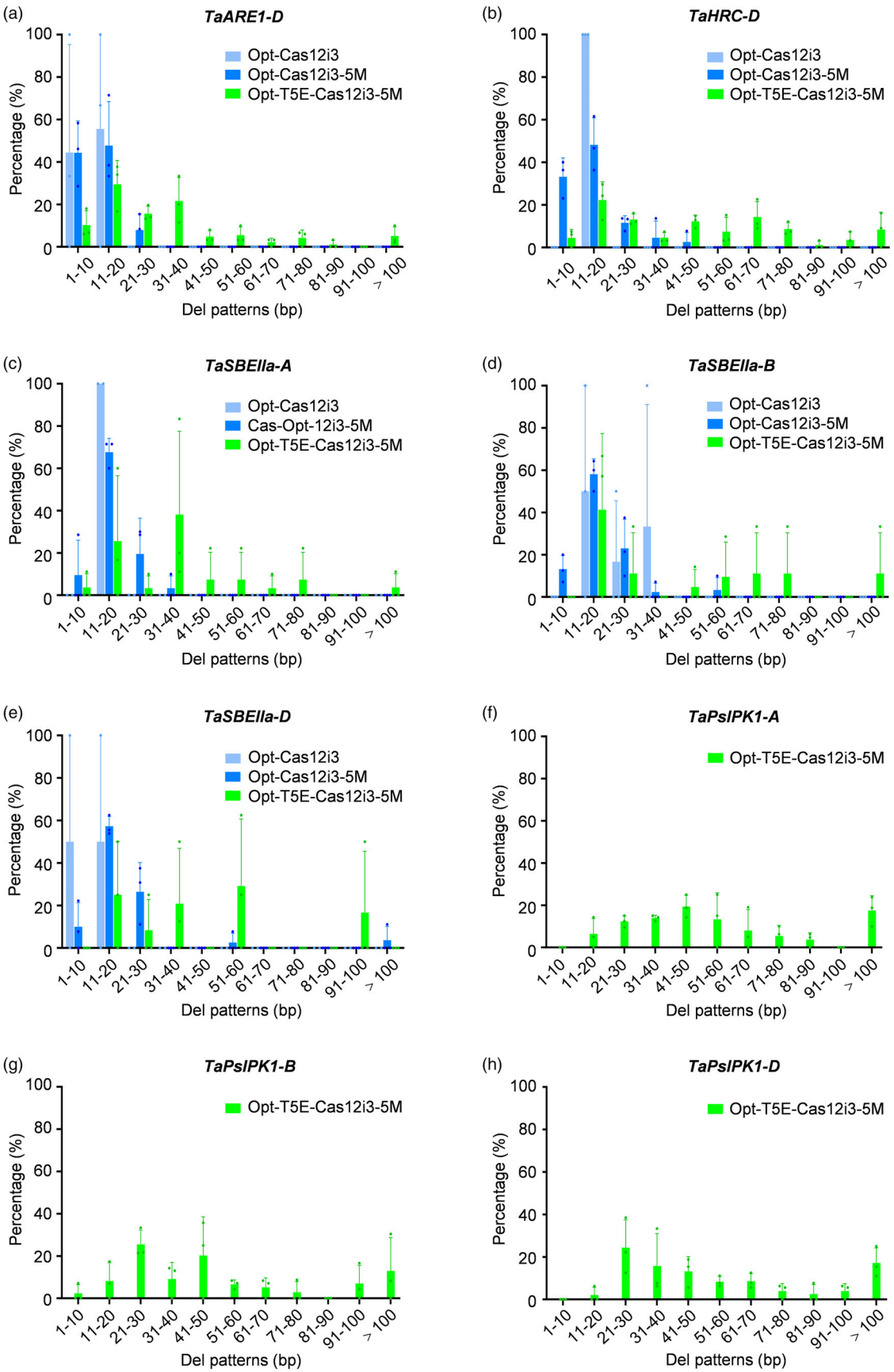

Figure 3 The deletion patterns induced by the Opt-Cas12i3, Opt-Cas12i3-5M and Opt-T5E-Cas12i3-5M at 8 targeted loci across four endogenous genes, respectively. The percentages of different deletion patterns induced by Opt-Cas12i3, Opt-Cas12i3-5M and Opt-T5E-Cas12i3-5M at (a) *TaARE1-D*, (b) *TaHRC-D*, (c) *TaSBEIIa-A*, (d) *TaSBEIIa-B* and (e) *TaSBEIIa-D* loci, respectively, and induced by Opt-T5E-Cas12i3-5M at (f) *TaPslPK1-A*, (g) *TaPslPK1-B* and (h) *TaPslPK1-D* loci, respectively.

Opt-T5E-Cas12i3-5M enables robust genome editing in different wheat varieties

Wheat genetic transformation and genome editing are usually genotype-dependent. To explore the feasibility and universality of the Opt-T5E-Cas12i3-5M strategy in other wheat varieties with different genetic backgrounds, we further investigated its editing efficiencies in two other Chinese elite wheat varieties, Zhengmai 1860 (ZM1860) and Zhengshi 9170 (ZS9170), at the endogenous *TaSBEIIa* target, respectively. For ZM1860, the editing efficiency was 70.00% (7/10) and 80.00% (4/5) in two transformation repeats, respectively, with the average editing efficiency of 75.00 ± 7.07% (Table 1). All the obtained 11 edited wheat lines carried mutations in the A, B and D subgenomes simultaneously. Among which, 54.55% (6/11) were homozygous mutant lines (Table S7). In all the indels induced by Opt-T5E-Cas12i3-5M, 28.38% were 1–30 bp deletions, 47.65% were 31–100 bp deletions, and 23.97% were larger than 100 bp deletions (Table S9). For ZS9170, the editing efficiency was 77.78% (7/9) and 75.00% (3/4) in two transformation repeats, respectively, with the average editing efficiency of 76.39 ± 1.97% (Table 1). In the obtained 10 independent edited wheat lines, one line had a mutation in the A subgenome and nine lines carried simultaneous mutations in the A, B and D subgenomes, respectively, among which four lines containing either homozygous or biallelic mutations in A, B and D subgenomes (Table S7). In all the indels induced by Opt-T5E-Cas12i3-5M, 41.10% were 1–30 bp deletions, 54.25% were 31–100 bp deletions, and 4.65% were larger than 100 bp deletions (Table S9).

Together, except ZM7698, Opt-T5E-Cas12i3-5M also enables robust genome editing in two different wheat varieties, ZM1860 and ZS9170. The establishment of the Opt-T5E-Cas12i3-5M system not only enriches the wheat genome editing toolkits but also will facilitate its wide application in wheat genetic improvement as well as other polyploidy crop species.

Inheritance and stability of the mutations and generation of transgene-free wheat mutant lines

To investigate whether the targeted mutagenesis generated through the Opt-T5E-Cas12i3-5M system could be transmitted to the next generation, we analysed the progenies of the T_0 lines at the T_1 generation. We selected T_1 progenies derived from either homologous, biallelic or heterozygous T_0 lines for further segregation analysis. All of the mutations detected in the tested T_0 lines were transmitted to the T_1 generation without the occurrence of new mutations (Table 2). For mutations that were homozygous in the T_0 generation, the transmission rates were 100%, and those mutations that were heterozygous in the T_0 generation segregated in a Mendelian fashion (homozygous/heterozygous/WT = 1:2:1) in the T_1 generation (Table 2). To determine whether plasmid DNA sequences were present in these mutant lines, we performed PCR amplification using the primer sets designed to specifically amplify *Cas12i3*, *crRNA* cassettes and *bar* sequences, respectively (Table 1). We successfully recovered *Cas12i3*, *crRNA* cassettes and *bar* transgene-free plants from the T_1 progenies of T_0 mutants (Table 2).

Following segregation, we successfully obtained a series of transgene-free mutant lines with triple-null *Tasbella* alleles in ZM7698 in the T_1 generation. Scanning electron microscopy (SEM) was used to determine morphological changes of the starch granules in mature endosperms of ZM7698 and these triple null mutant lines. As indicated in Figure 4, the starch granules of ZM7698 WT plants showed three typical types of granules (A-type, B-type and C-type), which were smooth and spherical to ellipsoidal in shape, whereas these from the *Tasbella* triple-null mutant lines had distorted granules with varying intensities compared to those of WT (Figure 4). Especially, the starch granules in *aabbdd* endosperms were highly irregular in shape, and a large proportion of A-type granules appeared to be sickle-shaped, which was the typical characteristic of wheat high in resistant starch, in consistence with our previous report (Li *et al.*, 2021b).

Off target analyses

To evaluate the specificity of Cas12i3, Cas12i3-5M and T5E-Cas12i3-5M in wheat stable lines with targeted mutagenesis, we further investigated if the off-target effects occurred in the mutant lines. Based on the predictions of the CRISPR RGEN Tools (http://www.rgenome.net/cas-offinder/), we identified several potential off-target sites of *TaARE1-D*, *TaHRC-D*, *TaSBEIIa* and *TaPslPK1* targets, respectively. We then used genome-specific PCR and Sanger sequencing to determine the potential off-target effects. Among the four target genes, we only detected off-target effects at the OFF-TaARE1-D site with efficiencies of 4.17%, and no mutations were detected at the other tested putative off-target loci in the wheat genome (Table S10).

Discussion

In this study, we report the engineering of a robust Opt-T5E-Cas12i3-5M-mediated genome editing system in wheat through fusion of T5E and in combination with an optimised crRNA expression strategy. We first demonstrated that fusion of T5E to the N-termini of Cas12i3-5M (T5E-Cas12i3-5M) could significantly improve its editing efficacy in HEK293 cells, even significantly higher than that of LbCas12a at the tested three target sites (Figure 1e). We then performed the wheat genome editing by using two different crRNA expression strategies (Figure 2a). Our results indicated that when using a conventional crRNA expression strategy, in which the expression of the DR-target-DR array was under the control of *TaU3*, the editing efficiencies of Cas12i3, Cas12i3-5M and T5E-Cas12i3-5M in wheat remain lower, with Cas12i3 and Cas12i3-5M inducing no targeted mutagenesis at all (Figure 2a, Table 1). We further optimised the crRNA expression strategy (Figure 2a). Our results demonstrated that Opt-T5E-Cas12i3-5M could significantly increase the editing efficiencies by up to 7.95-fold and 1.33-fold in comparison to Opt-Cas12i3 and Opt-Cas12i3-5M,

Table 2 Transmission and segregation of CRISPR/Cas12i3 and its variants induced target mutagenesis from T_0 to T_1 generation

The genotypes of analysed T_0 plants				The segregation of mutations in T_1 population					
Target Gene	Line ID	Genotype [a]	Induced mutations (bp) [b]	No. of T_1 plants detected	Genotype (Ho1: He: Ho2) [c]	Expected segregation ratio (Ho1: He: Ho2)	χ^2	P [d]	Cas12i3/ crRNA/bar [e]
TaARE1-D	Taare1-D-A23	dd	d19; d56	56	15:29:12	1:2:1	0.393	0.822**	48+: 8−
	Taare1-D-A48-2	Dd	d41; wt	36	7:19:10	1:2:1	0.611	0.737**	28+: 8−
	Taare1-D-A107	dd	d34; d37	33	8:19:6	1:2:1	1.000	0.607**	24+: 9−
TaHRC-D	Tahrc-D-H9	Dd	d23; wt	30	5:19:6	1:2:1	2.200	0.333*	25+: 5−
	Tahrc-D-H19	dd	d41	11					10+: 1−
TaSBEIIa	Tasbella-S5-1	Aa	d81; wt	20	7:6:7	1:2:1	3.200	0.202*	15+: 5−
		bb	d51; d22		5:12:3	1:2:1	1.200	0.549**	
		dd	d17; d78		6:10:4	1:2:1	0.400	0.819**	
	Tasbella-S6-1	aa	d22; d13	11	4:6:1	1:2:1	1.727	0.422*	10+: 1−
		bb	d12; d32		5:5:1	1:2:1	3.000	0.223*	
		dd	d34; d23		5:3:3	1:2:1	3.000	0.223*	
	Tasbella-S14	Aa	d26; wt	85	31:34:20	1:2:1	6.247	0.044	58+: 27−
		bb	d64; d62		22:45:18	1:2:1	0.671	0.715**	
		dd	d43; d37		22:40:23	1:2:1	0.318	0.853**	
	Tasbella-S37	aa	d58; d77	16	6:7:3	1:2:1	1.375	0.503**	16+: 0−
		Bb	wt; d116		4:10:2	1:2:1	1.500	0.472*	
		DD	wt						
	Tasbella-S41	Aa	wt; d79	11	4:5:2	1:2:1	0.818	0.664**	9+: 2−
		bb	d119; d76		3:6:2	1:2:1	0.273	0.873**	
		Dd	d97; wt		3:5:3	1:2:1	0.091	0.956**	

[a]The capital letters A, B, and D, and the lower-case letters a, b, and d, represent the wild-type and mutated alleles of a specific target gene in the A, B, and D subgenomes, respectively.

[b]WT, wild type; "d" indicates deletion of the indicated number of nucleotides.

[c]Ho 1, He and Ho 2, represents homozygote 1, heterozygote and homozygote 2, respectively.

[d]χ^2 test results are shown for the degree of agreement between the segregation of heterozygous lines and the Mendelian 1:2:1 ratio to be observed.

[e]"+" represents that Cas12i3/crRNA/Bar are detected, and "−" shows Cas12i3/crRNA/Bar are absent.

*0.1 < P < 0.5, in good agreement with 1:2:1.

**P > 0.5, in very good agreement with 1:2:1.

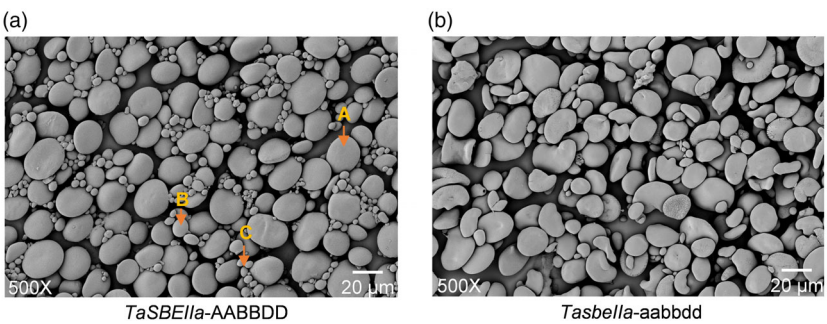

Figure 4 Starch granules of ZM7698 and its *Tasbella* mutant line. SEM observation of the purified starch granules in mature seeds from ZM7698 and its *Tasbella* mutant line. The starch granules were smooth, spherical to ellipsoidal in shape (a), while these from the *aabbdd* mutant line (b) were sickle-shaped and distorted granules at varying degrees, and less C-type starch granules. The arrows indicate different types of starch granules, respectively. A-type granule: >10 μm in diameter; B-type granule: 5–10 μm in diameter; C-type granule: <5 μm. The scale bar is 20 μm.

respectively, reaching average efficiencies ranging from 63.25% to 88.99% across four endogenous target genes in stable lines of three elite Chinese wheat varieties (Table 1). This is in consistence with a report in rice prime editing, where the optimised sgRNA expression strategy in which the 35S composite promoter was used to drive the expression of the tRNA-target-HDV array significantly improved the rice prime editing efficacy (Jiang *et al.*, 2022). To our knowledge, this is the first report of the successful application of Cas12i3-5M for robust genome editing in hexaploidy wheat with a complex genomic background. Given

the advantages of Cas12i3-5M with less restricted canonical 'TTN' PAM compared with LbCas12a/AsCas12a and of expanding the genome editing scope compared to SpCas9 with canonical 'NGG' PAM, in case of editing in AT-rich regions, especially genome editing in the 5′- and 3′-regulatory regions of the encoding genes, our robust Opt-T5E-Cas12i3-5M system reported in this study not only expands the editing scope and enriches the wheat genome editing toolkits but also will facilitate its application in genome editing of wheat as well as other agriculturally important polyploidy crop plants either for biological research or genetic improvement.

There is a series of studies reporting the fusion of exonucleases to CRISPR endonucleases, which in most cases leads to an increased rate of deletions with a higher proportion of larger deletions (Certo *et al*., 2012; Clements *et al*., 2017; He *et al*., 2024; Lainscek *et al*., 2022; Ordon *et al*., 2023; Weiss *et al*., 2020; Wu *et al*., 2020; Zhang *et al*., 2020b). Our results are in consistency with these previous reports. Here, we demonstrated that whereas Opt-Cas12i3 and Opt-Cas12i3-5M usually induced deletions with a majority of deletions less than 30 bp, Opt-T5E-Cas12i3-5M enabled a higher proportion of larger deletions across 8 target loci in wheat (Figure 2c, Figure 3). This is particularly valuable for genome editing of wheat and other polyploid crop species. As we described in the Introduction section, the high homology among these three subgenomes (AABBDD) of wheat may compromise the editing performances of Cas12i3-5M or other Cas12 family members due to the produced 5′-overhangs, which could potentially be repaired either by error-free NHEJ or using other uncut homologous subgenomes as repair templates. The performances of the natural and engineered variants of Cas12a (FnCas12a and LbCas12a) and Cas9 for their ability to induce mutations in endogenous genes controlling important agronomic traits were investigated in wheat. Whereas FnCas12a did not induce detectable mutations, LbCas12a exhibited a relatively lower editing efficiency in comparison to SpCas9 (Wang *et al*., 2021). In this study, the production of higher proportions of larger deletions by Opt-T5E-Cas12i3-5M may prevent the re-ligation of the DNA strand at the cleavage sites and disrupt the error-free NHEJ repair pathway, and thus significantly improve the editing efficiency. This will benefit the development of other genome editing toolkits, such as multiplex gene editing to pyramid several agronomically important genes as well as gene replacement in wheat, as both toolkits necessitate the higher DSB cutting activities (Li *et al*., 2021c; Luo *et al*., 2021; Wang *et al*., 2021). Besides, different 5′-exonucleases may have different activities in processing the resection of the 5′-end of the DNA strand at the cleavage sites (He *et al*., 2024; Schreiber *et al*., 2024). Next, it would be valuable to systematically evaluate the performances of different Exo-Cas12i3-5M fusions in the genome editing of wheat and other agriculturally important polyploid crop species.

In addition, like other Cas12i family members, Cas12i3-5M employed a 20 bp spacer in its crRNA with its cleavage sites located at 18 bp and 24 bp at the distal end of the PAM in the 5′-DNA strand and 3′-DNA strand, respectively (Bai *et al*., 2024; Chen *et al*., 2022; Duan *et al*., 2024; Lv *et al*., 2024). In this study, we used a 23 bp spacer in the crRNA of Cas12i3/Cas12i3-5M (Table S3) in order to compare with the performance of LbCas12a in HEK293T cells. The longer spacer sequence in crRNA might minimise the off-target effects. However, while no off-target effects were observed at the potential off-target loci of other target sequences, for *TaARE1-D*, of 72 independent lines tested, we observed 3 lines had the off-target editing at *TaARE1-A*, a homologue of *TaARE1-D* on subgenome 7A (Table S10). The off-target site has one 'T' instead of 'G' at position 15 at the distal end of the PAM (Table S10), indicating that 1–14 bp is probably the seed sequence of the crRNA spacer for Cas12i3-5M. However, the seed sequence of Cas12i3-5M needs to be further evaluated by using more mutated targets *in vitro* or more endogenous targets *in vivo* in stable lines.

In summary, we successfully engineered a robust Opt-T5E-Cas12i3-5M-mediated genome editing system in wheat through the fusion of T5E and in combination with an optimised crRNA expression strategy. Our robust Opt-T5E-Cas12i3-5M system reported in this study not only expands the editing scope and enriches the wheat genome editing toolkits but also will facilitate its application in genome editing of wheat and other agriculturally important polyploidy as well as transformation-recalcitrant crop plants, either for biological research or genetic improvement.

Materials and methods

Construction of the knockout vectors

The basic vector S4254 and P4190 vector used in this study were kindly provided by Dr. Zhiqiang Duan from Shandong BellaGen Biotechnology Co., Ltd. The S4254 vector contains a codon-optimised Cas12i3, which carries two nuclear location signals (NLS), and the NLS-Cas12i3-NLS-T2A-BFP cassette is driven by the CMV promoter. crRNA is promoted by the pol III U6 promoter. P4190 vector contains the EGFxxFP reporter system used for detecting the editing efficiency of Cas12i3in HEK293T cells. In the reporter system, the mCherry-T2A-EGFxxFP is driven by the EF-1α core promoter, and the PAM-Target sequences are inserted inside the EGFP to disrupt its fluorescence. Targeted cleavage in the inserted sequence can restore EGFP fluorescence through single-strand annealing (SSA)-mediated DNA repair between the repeats of EGFxxFP. P4190 and S4254 in this system can constitutively express mCherry and BFP fluorescence, respectively.

The NLS-*Avr*II-BFP-NLS fragment was obtained through overlapping PCR and cloned into the *Sac*I-digested S4254 plasmid using a seamless cloning assembly kit for constructing the vector S4254-CMV promoter-NLS-*Avr*II-BFP-NLS-ter (TransGen Biotech, Beijing, China). For S4254-CMV promoter-NLS-*Avr*II-BFP-NLS-ter-Actin-tRNA-*Asc*I-HDV-ter, the Chicken Actin-tRNA-*Asc*I-HDV-ter was cloned into *Spe*I and *Ssp*I-digested S4254-CMV promoter-NLS-*Avr*II-BFP-NLS-ter. Fragments of Cas12a, Cas12i3, Cas12i3-5M, ExoI-Cas12i3-5M and T5E-Cas12i3-5M were obtained by PCR amplification. The S4254-CMV promoter-NLS-Cas12i3-NLS-T2A-BFP-ter-Actin-tRNA-*Asc*I-HDV-ter (S4254-Cas12a), S4254-CMV promoter-NLS-Cas12i3-NLS-T2A-BFP-ter-Actin-tRNA-*Asc*I-HDV-ter (S4254-Cas12i3), S4254-CMV promoter-NLS-Cas12i3-5M-NLS-T2A-BFP-ter-Actin-tRNA-*Asc*I-HDV-ter (S4254-Cas12i3-5M), S4254-CMV promoter-NLS-ExoI-Cas12i3-5M-NLS-T2A-BFP-ter-Actin-tRNA-*Asc*I-HDV-ter (S4254-ExoI-Cas12i3-5M) and S4254-CMV promoter-NLS-T5E-Cas12i3-5M-NLS-T2A-BFP-ter-Actin-tRNA-*Asc*I-HDV-ter (S4254-T5E Cas12i3-5M) were obtained by cloning Cas12a, Cas12i3, Cas12i3-5M, ExoI-Cas12i3-5M and T5E-Cas12i3-5M into *Avr*II digested S4254-CMV promoter-NLS-*Avr*II-BFP-NLS-ter-Actin-tRNA-*Asc*I-HDV-ter, individually. Furthermore, we investigated the editing performances of LbCas12a, Cas12i3, Cas12i3-5M, ExoI-Cas12i3-5M and T5E-Cas12i3-5M at the *TaARE-D*, *TaHRC-D* and *TaSBEIIa* targets, respectively. The spacers were designed by targeting the

encoding region of the D genome of *the TaARE* gene (Zhang *et al*., 2021), D genome of the *TaHRC* gene (Su *et al*., 2019) and the three subgenomes of the *TaSBEIIa* gene (Li *et al*., 2021b), respectively (Figure 1c). For Cas12a-TaARE-D/TaHRC-D/TaSBEIIa, Cas12i3-TaARE-D/TaHRC-D/TaSBEIIa, Cas12i3-5M-TaARE-D/TaHRC-D/ TaSBEIIa, Exo1-Cas12i3-5M-TaARE-D/TaHRC-D/TaSBEIIa and T5E-Cas12i3-5M-TaARE-D/TaHRC-D/TaSBEIIa, the crRNAs targeting *TaARE-D*, *TaHRC-D* and *TaSBEIIa* loci were cloned into S4254-Cas12a, S4254-Cas12i3, S4254-Cas12i3-5M, S4254-Exol-Cas12i3-5M and S4254-T5E Cas12i3-5M, individually. The 'TaARE-D target-random sequence1-TaHRC-D-random sequence 2-TaSBEIIa-random sequence 3' fragment was cloned into the "xx" of EGFxxFP (P4190-wheat). The Cas12a-TaARE-D/TaHRC-D/TaSBEIIa, Cas12i3-TaARE-D/TaHRC-D/ TaSBEIIa, Cas12i3-5M-TaARE-D/TaHRC-D/TaSBEIIa, Exol-Cas12i3-5M-TaARE-D/TaHRC-D/TaSBEIIa and T5E-Cas12i3-5M-TaARE-D/TaHRC-D/TaSBEIIa, together with P4190-wheat, were used for analysing the editing efficiency in HEK293T cells.

The basic vector pBUE411-Ubi-NLS-Cas9-NLS-E9-35S-Bar (pBUE411-Cas9) vector used in this study was kindly provided by Profs. Qijun Chen and Zhongfu Ni from China Agriculture University. This vector contains a codon-optimised Cas9 that carries two nuclear location signals and is driven by the *ubiquitin* gene promoter of maize (*Zea mays* L.). In pBUE411-Cas9, the *bar* gene, used for callus selection in the wheat tissue culture, is driven by the 35S promoter. The vector pHUE411-Ubi-NLS-Cas9-NLS-E9-35S-HptII (pHUE411-Cas9) was constructed based on the pBUE411-Cas9 vector by replacing the *bar* gene with a hygromycin-resistant gene (*hptII*) using the pEASY-Uni Seamless Cloning and Assembly Kit (TransGen Biotech, Beijing, China).

The pHUE411-Cas12i3 and pHUE411-Cas12i3-5M used in the study were constructed by replacing Cas9 in pHUE411-Cas9 with Cas12i3 and Cas12i3-5M, individually. The pHUE411-T5E-Cas12i3-5M were constructed by fusing T5 Exonuclease to the N-Terminal of Cas12i3-5M in vector pHUE411-Cas12i3-5M. A cassette for TaU3-driven crRNA expression targeting *TaARE1* loci was obtained by overlap PCR and inserted into the *Pme*I-digested pHUE411-Cas12i3, pHUE411-Cas12i3-5M, and pHUE411-T5E-Cas12i3-5M to construct Cas12i3, Cas12i3-5M and T5E-Cas12i3-5M, individually.

The pBUE411-Cas12i3 and pBUE411-Cas12i3-5M constructs were obtained by replacing Cas9 in pHUE411-Cas9 with Cas12i3 and Cas12i3-5M, respectively. The pBUE411-T5E-Cas12i3-5M and were constructed by fusing T5 Exonuclease to the N-Terminal of the Cas12i3-5M protein in pBUE411-T5E-Cas12i3-5M. A cassette for 35S composite (35S-CmYLCV-U6)-driven crRNA expression was obtained by overlap PCR and inserted into the *Pme*I-digested pBUE411-Cas12i3, pBUE411-Cas12i3-5M and pBUE411-T5E-Cas12i3-5M. The double strands of protospacers targeting *TaARE-D*, *TaHRC-D* and *TaSBEIIa* loci were synthesised, annealed and inserted into *Pme*I-digested pBUE411-Cas12i3, pBUE411-Cas12i3-5M, and pBUE411-T5E-Cas12i3-5M to construct Opt-Cas12i3-TaARE-D/TaHRC-D/TaSBEIIa, Opt-Cas12i3-5M-TaARE-D/TaHRC-D/ TaSBEIIa and Opt-T5E-Cas12i3-5M-TaARE-D/TaHRC-D/TaSBEIIa, individually. Also, the double strands of protospacers targeting the *TaPsIPK* locus *Pme*I digested pBUE411-T5E-Cas12i3-5M to construct Opt-T5E-Cas12i3-5M-TaPsIPK. All vectors were confirmed by Sanger sequencing (TSINGKE, Beijing, China). A one-step cloning kit (ClonExpress II One Step Cloning Kit, Vazyme, Beijing, China) was used for vector' construction. All the primers used during these construction steps are as listed in Table S1.

Cell culture, transfection, and flow cytometry analysis

HEK293T cells were cultured in high-glucose DMEM supplemented with 10% (v/v) foetal bovine serum (10 099 141; Gibco, Grand Island, USA) and 1% penicillin/streptomycin (15 140 122; Gibco, NY, USA) at 37 °C with 5% CO_2. HEK293T cells were seeded into 12-well plates and transfected at ~80% confluency. For all of the transfections, 2.0 μg plasmid was mixed with 100 μL Opti-MEM (51 985 091; Gibco, NY, USA) and then combined with a solution comprising 100 μL Opti-MEM and 3 μL Lipofectamine 2000 (11 668-019; Invitrogen). The resulting DNA/Lipofectamine mixture was then added to the cells after incubating for 15 min at room temperature. Transformed cells were then incubated for After 5 h of transformation, 1000 μL of Opti-MEM medium was exchanged in each transfected well with DMEM supplemented with 10% (v/v) foetal bovine serum and 1% penicillin/streptomycin. Cells were then incubated for an additional 48 h before being harvested for flow cytometry. Transfected cells of each well were digested with 500 μL of 0.25% trypsin (25 200-056; Gibco, NY, USA) after removing the medium. Then, 1000 μL of medium was added to terminate the digestion, and the cells were resuspended in 500 μL of medium after 3 min of centrifugation at 1000 rpm. Cells were then pipetted into a 5-mL round-bottom polystyrene test tube with a cell strainer snap cap (352 235; Corning, NY, USA) and kept on ice. Flow cytometry data were collected using a CytoFLEX (Beckman Coulter Life Sciences, California, USA) and analysed using CyExpert version 2.5.0.77 software. For the assay of mutations in the target sites of endogenous genes, cells were sorted using BD FACSAria SORP.

Agrobacterium-mediated wheat transformation

The constructed vectors were introduced into *Agrobacterium tumefaciens* strain EHA105 using the freeze–thaw method. The colony of the *A. tumefaciens* strain was then grown in liquid LB medium (containing 100 mg/L kanamycin and 25 mg/L rifampicin) at 28 °C with shaking. After overnight incubation, 20 μL of each culture was transferred to 2 mL of fresh Mgl medium and incubated at 28 °C with shaking until the OD600 reached 0.6 ~ 1.0. The cells were harvested by centrifugation at 4200 g for 10 min and then adjusted to an OD600 of 0.6 with Inf medium. The embryos derived from cultivars ZM7698, ZM1860, and ZS9170 were carefully placed in a sterile tube and were incubated with the Agrobacterium strains for 5 min. After incubation, the embryos were transferred onto AS medium and co-cultivated for 2 days in the dark at 25 °C. After co-cultivation process, the embryos were put on resting medium for one week with hypocotyls excised and then were selected on medium containing 5 and 10 mg/L phosphinothricin for 2 weeks in dark at 25 °C, respectively. Then the grown calli were transferred to regeneration media to generate green plants in light at 25 °C (16L:8D).

Molecular characterisation of the edited plants

Wheat genomic DNA from approximately 0.2 g of leaf tissue was extracted using a DNA Quick Plant System (Tiangen, Beijing, China). PCR amplification was performed using rTaq polymerase with 200 ng of genomic DNA as a template. All plants were further genotyped individually by PCR and DNA Sanger sequencing, and the sequencing results were analysed using DsDecode (http://skl.scau.edu.cn/dsdecode/) (Liu *et al*., 2015). Some PCR products were also cloned into the TA cloning vector P-easy (TransGen Biotech, Beijing, China), and 12 positive colonies for each sample were sequenced.

Off-target analysis

To investigate off-target effects, we selected several potential off-target sites for each target, based on NCBI (https://www.ncbi.nlm.nih.gov/) and CRISPR RGEN Tools (http:// www.rgenome.net/cas-offinder/). Site-specific genomic PCR and Sanger sequencing were used to determine the off-target effects. The primer sets were as listed in Table S1.

Segregation and statistical analysis

Genomic DNAs were extracted from T_1 seedlings using a DNA Quick Plant System (Tiangen, Beijing, China) from leaf tissues. PCR amplification was performed using EASY Taq polymerase (TransGen Biotech, Beijing, China) and 200 ng of genomic DNA as a template. The PCR products were directly sequenced to perform segregation analysis of mutation events in T_1 seedlings (Table S1). The PCR amplification was used to detect *Cas12i3*, *crRNA* cassettes and *bar* sequences in T_1 seedlings. A χ^2 test was performed to test whether the segregations of edited events were somatic and in accordance with Mendelian genetics.

Acknowledgements

We apologise to those whose work we were unable to cite due to space and reference limitations. This work is partly funded by the National Key Research and Development Program of China (Grant No. 2021YFF1000204 to L.X.), National Natural Science Foundation of China (Grant No. 32188102 to L.X.), Biological Breeding-Major Projects (Grant No. 2023ZD04074 to S.L.), Hainan Seed Industry Lab (Grant No. B23CJ0208 to L.X.), and National Engineering Research Centre of Crop Molecular Breeding.

Conflict of interest

A patent application was filed based on the results reported in this paper. All the authors declare no competing financial interests.

Author contributions

LX conceived the project. WW, SL, LY, CZ, JL and YH performed the experiments. SL and WW wrote the manuscript. LX revised the manuscript. All the authors read the final version of this manuscript.

Data availability statement

The data that supports the findings of this study are available in the supplementary material of this article.

References

Bai, Y.H., Liu, S.N., Bai, Y., Xu, Z.S., Zhao, H.N., Zhao, H.M., Lai, J.S. *et al.* (2024) Application of CRISPR/Cas12i.3 for targeted mutagenesis in *Broomcorn millet* (L.). *J. Integr. Plant Biol.* **66**, 1544–1547.

Bigelyte, G., Young, J.K., Karvelis, T., Budre, K., Zedaveinyte, R., Djukanovic, V., Van Ginkel, E. *et al.* (2021) Miniature type V-F CRISPR-Cas nucleases enable targeted DNA modification in cells. *Nat. Commun.* **12**, 6191.

Budman, J., Kim, S.A. and Chu, G. (2007) Processing of DNA for nonhomologous end-joining is controlled by kinase activity and XRCC4/Ligase IV. *J. Biol. Chem.* **282**, 11950–11959.

Certo, M.T., Gwiazda, K.S., Kuhar, R., Sather, B., Curinga, G., Mandt, T., Brault, M. *et al.* (2012) Coupling endonucleases with DNA end-processing enzymes to drive gene disruption. *Nat. Methods* **9**, 973–975.

Chen, Y., Hu, Y., Wang, X., Luo, S., Yang, N., Chen, Y., Li, Z. *et al.* (2022) Synergistic engineering of CRISPR-Cas nucleases enables robust mammalian genome editing. *Innovation* **3**, 100264.

Clements, T.P., Tandon, B., Lintel, H.A., McCarty, J.H. and Wagner, D.S. (2017) RICE CRISPR: rapidly increased cut ends by an exonuclease Cas9 fusion in zebrafish. *Genesis* **55**, e23044.

Duan, Z.Q., Liang, Y.F., Sun, J.L., Zheng, H.J., Lin, T., Luo, P.Y., Wang, M.G. *et al.* (2024) An engineered Cas12i nuclease that is an efficient genome editing tool in animals and plants. *Innovation* **5**, 100564.

Garforth, S.J. and Sayers, J.R. (1997) Structure-specific DNA binding by bacteriophage T5 5′->3′ exonuclease. *Nucleic Acids Res.* **25**, 3801–3807.

Gu, J.F., Lu, H.H., Tippin, B., Shimazaki, N., Goodman, M.F. and Lieber, M.R. (2007) XRCC4:DNA ligase IV can ligate incompatible DNA ends and can ligate across gaps. *EMBO J.* **26**, 1010–1023.

He, Y., Han, Y., Ma, Y., Liu, S., Fan, T., Liang, Y., Tang, X. *et al.* (2024) Expanding plant genome editing scope and profiles with CRISPR-FrCas9 systems targeting palindromic TA sites. *Plant Biotechnol. J.* **22**, 2488–2503.

Huang, X., Sun, W., Cheng, Z., Chen, M.X., Li, X.Y., Wang, J.Y., Sheng, G. *et al.* (2020) Structural basis for two metal-ion catalysis of DNA cleavage by Cas12i2. *Nat. Commun.* **11**, 5241.

Hui, F.J., Tang, X., Li, B., Alariqi, M., Xu, Z.P., Meng, Q.Y., Hu, Y.X. *et al.* (2024) Robust CRISPR/Mb2Cas12a genome editing tools in cotton plants. *Imeta.* **3**, e209.

Jiang, Y.Y., Chai, Y.P., Lu, M.H., Han, X.L., Lin, Q.P., Zhang, Y., Zhang, Q. *et al.* (2020) Prime editing efficiently generates W542L and S621I double mutations in two ALS genes in maize. *Genome Biol.* **21**, 257.

Jiang, Y.Y., Chai, Y.P., Qiao, D.X., Wang, J.Y., Xin, C.P., Sun, W., Cao, Z.H. *et al.* (2022) Optimized prime editing efficiently generates glyphosate-resistant rice plants carrying homozygous TAP-IVS mutation in. *Mol. Plant* **15**, 1646–1649.

Karmakar, S., Panda, D., Panda, S., Dash, M., Saha, R., Das, P., Avinash, S.P. *et al.* (2024) A miniature alternative to Cas9 and Cas12: transposon-associated TnpB mediates targeted genome editing in plants. *Plant Biotechnol. J.* **22**, 2950–2953.

Lainscek, D., Forstneric, V., Mikolic, V., Malensek, S., Pecan, P., Bencina, M., Sever, M. *et al.* (2022) Coiled-coil heterodimer-based recruitment of an exonuclease to CRISPR/Cas for enhanced gene editing. *Nat. Commun.* **13**, 3604.

Li, B., Liang, S.J., Alariqi, M., Wang, F.Q., Wang, G.Y., Wang, Q.Q., Xu, Z.P. *et al.* (2021a) The application of temperature sensitivity CRISPR/LbCpf1 (LbCas12a) mediated genome editing in allotetraploid cotton (*G. hirsutum*) and creation of nontransgenic, gossypol-free cotton. *Plant Biotechnol. J.* **19**, 221–223.

Li, B., Rui, H.P., Li, Y.J., Wang, Q.Q., Alariqi, M., Qin, L., Sun, L. *et al.* (2019) Robust CRISPR/Cpf1 (Cas12a)-mediated genome editing in allotetraploid cotton (*G. hirsutum*). *Plant Biotechnol. J.* **17**, 1862–1864.

Li, J., Jiao, G., Sun, Y., Chen, J., Zhong, Y., Yan, L., Jiang, D. *et al.* (2021b) Modification of starch composition, structure and properties through editing of TaSBEIIa in both winter and spring wheat varieties by CRISPR/Cas9. *Plant Biotechnol. J.* **19**, 937–951.

Li, J.Y., Zhang, C., He, Y.B., Li, S.Y., Yan, L., Li, Y.C., Zhu, Z.W. *et al.* (2023) Plant base editing and prime editing: the current status and future perspectives. *J. Integr. Plant Biol.* **65**, 444–467.

Li, S., Zhang, C., Li, J., Yan, L., Wang, N. and Xia, L. (2021c) Present and future prospects for wheat improvement through genome editing and advanced technologies. *Plant Commun.* **2**, 100211.

Li, S., Zhang, X., Wang, W., Guo, X., Wu, Z., Du, W., Zhao, Y. *et al.* (2018) Expanding the scope of CRISPR/Cpf1-mediated genome editing in rice. *Mol. Plant* **11**, 995–998.

Li, S.Y., Zhang, Y.X., Xia, L.Q. and Qi, Y.P. (2020) CRISPR-Cas12a enables efficient biallelic gene targeting in rice. *Plant Biotechnol. J.* **18**, 1351–1353.

Li, Y.C., Li, S.Y., Li, C.F., Zhang, C., Yan, L., Li, J.Y., He, Y.B. *et al.* (2024) Fusion of a rice endogenous-methylpurine DNA glycosylase to a plant adenine base transition editor ABE8e enables A-to-K base editing in rice plants. *aBIOTECH* **5**, 127–139.

Liu, S., Sretenovic, S., Fan, T., Cheng, Y., Li, G., Qi, A., Tang, X. *et al.* (2022) Hypercompact CRISPR-Cas12j2 (CasPhi) enables genome editing, gene activation, and epigenome editing in plants. *Plant Commun.* **3**, 100453.

Liu, W., Xie, X., Ma, X., Li, J., Chen, J. and Liu, Y.G. (2015) DSDecode: a web-based tool for decoding of sequencing chromatograms for genotyping of targeted mutations. *Mol. Plant* **8**, 1431–1433.

Luo, J., Li, S., Xu, J., Yan, L., Ma, Y. and Xia, L. (2021) Pyramiding favorable alleles in an elite wheat variety in one generation by CRISPR-Cas9-mediated multiplex gene editing. *Mol. Plant* **14**, 847–850.

Lv, P., Su, F., Chen, F.Y., Yan, C.X., Xia, D.D., Sun, H., Li, S.S. *et al*. (2024) Genome editing in rice using CRISPR/Cas12i3. *Plant Biotechnol. J.* **22**, 379–385.

Ma, G.G., Yan, F., Ren, B., Lu, Z.W., Xu, H., Wu, F.X., Li, S.F. *et al*. (2024) LbCas12a-nuclease-mediated tiling deletion for large-scale targeted editing of non-coding regions in rice. *Plant Commun.* **5**, 100815.

Moore, J.K. and Haber, J.E. (1996) Cell cycle and genetic requirements of two pathways of nonhomologous end-joining repair of double-strand breaks in Saccharomyces cerevisiae. *Mol. Cell. Biol.* **16**, 2164–2173.

Ordon, J., Kiel, N., Becker, D., Kretschmer, C., Schulze-Lefert, P. and Stuttmann, J. (2023) Targeted gene deletion with Cas9 and multiple guide RNAs in: four are better than two. *Plant Methods* **19**, 30.

Schindele, P. and Puchta, H. (2020) Engineering CRISPR/Cas12a for highly efficient, temperature-tolerant plant gene editing. *Plant Biotechnol. J.* **18**, 1118–1120.

Schreiber, T., Prange, A., Schäfer, P., Iwen, T., Grützner, R., Marillonnet, S., Lepage, A. *et al*. (2024) Efficient scar-free knock-ins of several kilobases in plants by engineered CRISPR-Cas endonucleases. *Mol. Plant* **17**, 824–837.

Shevelev, I.V., Belyakova, N.V., Kravetskaya, T.P. and Krutyakov, V.M. (2002) The correcting role of autonomous 3′→5′ exonucleases contained in mammalian multienzyme DNA polymerase complexes. *Mol. Biol.* **36**, 857–863.

Su, Z., Bernardo, A., Tian, B., Chen, H., Wang, S., Ma, H., Cai, S. *et al*. (2019) A deletion mutation in TaHRC confers Fhb1 resistance to Fusarium head blight in wheat. *Nat. Genet.* **51**, 1099–1105.

Sun, Y., Jiao, G., Liu, Z., Zhang, X., Li, J., Guo, X., Du, W. *et al*. (2017) Generation of high-amylose rice through CRISPR/Cas9-mediated targeted mutagenesis of starch branching enzymes. *Front. Plant Sci.* **8**, 298.

Tang, X., Lowder, L.G., Zhang, T., Malzahn, A.A., Zheng, X., Voytas, D.F., Zhong, Z. *et al*. (2017) A CRISPR-Cpf1 system for efficient genome editing and transcriptional repression in plants. *Nat Plants.* **3**, 17018.

Tong, H., Wang, X., Liu, Y., Liu, N., Li, Y., Luo, J., Ma, Q. *et al*. (2023) Programmable A-to-Y base editing by fusing an adenine base editor with an N-methylpurine DNA glycosylase. *Nat. Biotechnol.* **41**, 1080–1084.

Tran, P.T., Erdeniz, N., Symington, L.S. and Liskay, R.M. (2004) EXO1-A multi-tasking eukaryotic nuclease. *DNA Repair* **3**, 1549–1559.

Wang, N., Tang, C., Fan, X., He, M., Gan, P., Zhang, S., Hu, Z. *et al*. (2022) Inactivation of a wheat protein kinase gene confers broad-spectrum resistance to rust fungi. *Cell* **185**, 2961–2974.e19.

Wang, W., Tian, B., Pan, Q.L., Chen, Y.Y., He, F., Bai, G.H., Akhunova, A. *et al*. (2021) Expanding the range of editable targets in the wheat genome using the variants of the Cas12a and Cas9 nucleases. *Plant Biotechnol. J.* **19**, 2428–2441.

Weiss, T., Wang, C., Kang, X., Zhao, H., Elena Gamo, M., Starker, C.G., Crisp, P.A. *et al*. (2020) Optimization of multiplexed CRISPR/Cas9 system for highly efficient genome editing in Setaria viridis. *Plant J.* **104**, 828–838.

Wolter, F. and Puchta, H. (2019) Gene targeting can be enhanced by the use of CRISPR/Cas12a. *Plant J.* **100**, 1083–1094.

Wu, Y.Q., Yuan, Q.C., Zhu, Y.F., Gao, X., Song, J.B. and Yin, Z.R. (2020) Improving FnCas12a genome editing by exonuclease fusion. *Crispr J.* **3**, 503–511.

Xin, C.P., Qiao, D.X., Wang, J.Y., Sun, W., Cao, Z.H., Lu, Y., Jiang, Y.Y. *et al*. (2024) Enhanced editing efficiency in Arabidopsis with a LbCas12a variant harboring D156R and E795L mutations. *aBIOTECH* **5**, 117–126.

Yang, Y., Liu, S.C., Cheng, Y.Y., Nie, L.Y., Lv, C., Wang, G., Zhang, Y. *et al*. (2016) Highly efficient and rapid detection of the cleavage activity of Cas9/gRNA via a fluorescent reporter. *Appl. Biochem. Biotechnol.* **180**, 655–667.

Zetsche, B., Gootenberg, J.S., Abudayyeh, O.O., Slaymaker, I.M., Makarova, K.S., Essletzbichler, P., Volz, S.E. *et al*. (2015) Cpf1 is a single RNA-guided endonuclease of a class 2 CRISPR-Cas system. *Cell* **163**, 759–771.

Zhang, H., Li, Z., Xiao, R. and Chang, L. (2020a) Mechanisms for target recognition and cleavage by the Cas12i RNA-guided endonuclease. *Nat. Struct. Mol. Biol.* **27**, 1069–1076.

Zhang, H.N., Kong, X.F., Xue, M.X., Hu, J., Wang, Z.K., Wei, Y.H., Li, G.L. *et al*. (2023a) An engineered xCas12i with high activity, high specificity and broad PAM range. *Mol. Ther.* **31**, 253.

Zhang, J., Zhang, H., Li, S., Li, J., Yan, L. and Xia, L. (2021) Increasing yield potential through manipulating of an ARE1 ortholog related to nitrogen use efficiency in wheat by CRISPR/Cas9. *J. Integr. Plant Biol.* **63**, 1649–1663.

Zhang, L.Y., Li, G., Zhang, Y.X., Cheng, Y.H., Roberts, N., Glenn, S.E., DeZwaan-McCabe, D. *et al*. (2023b) Boosting genome editing efficiency in human cells and plants with novel LbCas12a variants. *Genome Biol.* **24**, 102.

Zhang, Q.W., Yin, K.Q., Liu, G.W., Li, S.N., Li, M.O. and Qiu, J.L. (2020b) Fusing T5 exonuclease with Cas9 and Cas12a increases the frequency and size of deletion at target sites. *Sci. China Life Sci.* **63**, 1918–1927.

Zhang, R., Tang, X., He, Y., Li, Y., Wang, W., Wang, Y., Wang, D. *et al*. (2024) IsDge10 is a hypercompact TnpB nuclease that confers efficient genome editing in rice. *Plant Commun.* **21**, 101068.

Zhong, Z., Zhang, Y., You, Q., Tang, X., Ren, Q., Liu, S., Yang, L. *et al*. (2018) Plant genome editing using FnCpf1 and LbCpf1 nucleases at redefined and altered PAM sites. *Mol. Plant* **11**, 999–1002.

Zhou, J.P., Liu, G.Q., Zhao, Y.X., Zhang, R., Tang, X., Li, L., Jia, X.Y. *et al*. (2023) An efficient CRISPR-Cas12a promoter editing system for crop improvement. *Nat Plants.* **9**, 588–604.

Supporting information

Additional supporting information may be found online in the Supporting Information section at the end of the article.

Table S1 The primer sets used in this study.
Table S2 Editing efficacies of Cas12a, Cas12i3, Cas12i3-5M, ExoI-Cas12i3-5M and T5E-Cas12i3-5M in HEK293T cells.
Table S3 The sequences of targets used in this study.
Table S4 Genotyping of the *Taare1* mutant lines generated by T5E-Cas12i3-5M in T_0 generation.
Table S5 Genotyping of ZM7698 *Taare1-D* mutant lines in T_0 generation.
Table S6 Genotyping of ZM7698 *Tahrc-D* mutant lines in T_0 generation.
Table S7 Genotyping of *Tasbella* mutant lines in T_0 generation.
Table S8 Genotyping of ZM7698 *Tapsipk1* mutant lines in T_0 generation.
Table S9 Indel patterns induced by Opt-Cas12i3, Opt-Cas12i3-5M, and Opt-T5E-Cas12i3-5M at three targets in wheat stable lines.
Table S10 Analysis of potential off-target effects.